Ni_2P/MCM-41 촉매의 구조와 촉매성능

이용걸*, 조계성, 전진우, S. Ted Oyama[1]
단국대학교 화학공학과, [1]버지니아공대 화학공학과
(yolee@dankook.ac.kr*)

Structure and Catalytic Performance of Ni_2P/MCM-41 Catalysts

Yong-Kul Lee*, Kye-Sung Cho, Jin-Woo Jun, S. Ted Oyama[1]
Department of Chemical Engineering, [1]Department of Chemical Engineering, Virginia Tech
(yolee@dankook.ac.kr*)

Introduction

Environmental regulations for reducing motor vehicle emissions has put considerable pressure on the refining industry worldwide to produce cleaner fuels, and has motivated much research for the development of new hydrotreating catalysts. Among alternatives to the widely used sulfides are transition-metal carbides, nitrides, and phosphides (1,2,3,4). Metal phosphides are a novel catalyst group for deep hydrotreating and have received much attention due to their high activity for hydrodesulfurization (HDS) and hydrodenitrogenation (HDN) of petroleum feedstocks (4,5,6,8). Previous studies of silica-supported Ni_2P employed a low surface area (90 $m^2 g^{-1}$) support (6,7). It is the objective of this work to investigate a mesoporous siliceous material (790 $m^2 g^{-1}$) as support. Particular attention is placed on understanding the effect of nitrogen, sulfur and aromatic compounds on the catalytic behavior, as these compounds are reported to inhibit HDS. The present study also includes the use of X-ray absorption fine structure (XAFS) spectroscopy to study the structure of the finely dispersed phosphide phases before and after reaction. As will be shown the samples after use show evidence for the formation of a surface phospho-sulfide phase of very high activity.

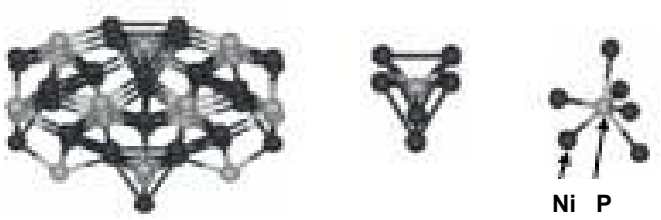

Figure 1. Local structure of Ni_2P with two types of trigonal prisms.

Experimental

Commercial SiO_2 supports (Cabot, Cab-O-Sil) of low surface area (L-90, 90 $m^2 g^{-1}$) was used as received. A mesoporous MCM-41 silica support was synthesized following a literature procedure (9). The supported Ni_2P catalysts were prepared with excess phosphorus (Ni/P=1/2) and a loading of 1.16 mmol Ni/g support (12.2 wt.% Ni_2P/SiO_2). Previous studies (6,7) had shown that this composition and loading level gave high activity and stability in hydroprocessing reactions. Samples prepared with low surface area silica (L90) were denoted as Ni_2P/SiO_2-L. The synthesis of the catalyst involved two steps (4,6,7). In the first step, a supported nickel phosphate precursor was prepared by incipient wetness impregnation of a solution of nickel nitrate and ammonium phosphate, followed by calcination at 673 K. In the second step, the supported metal phosphate was reduced to a phosphide by temperature-programmed reduction (TPR). In catalyst preparation, larger batches using up to 5.50 g of supported nickel phosphate were prepared in a similar manner by reduction to 873 K and 893 K for Ni_2P/SiO_2-L and Ni_2P/MCM-41, respectively. Sulfided Ni-Mo/Al_2O_3 (CR 424) was used as reference.

The prepared catalysts were characterized by XRD, N_2 adsorption and CO chemisorption. Also, X-ray absorption (XAS) spectra at the Ni K edge (8.333 keV) of reference and catalyst samples were recorded in the energy range 8.233 to 9.283 keV using synchrotron radiation at the National Synchrotron Light Source (NSLS) at Brookhaven National Laboratory (BNL), beamline X18B.

Hydrotreating was carried out at 3.1 MPa (450 psig) at two different temperatures, 573 K (300 ^oC) and 613 K (340 ^oC) in a three-phase upflow fixed-bed reactor. The feed liquid was prepared by combining different quantities of tetralin (Aldrich, 99%), n-tridecane (Alfa Aesar, 99%), quinoline (Aldrich, 99%), 4,6-dimethyldibenzo-thiophene (4,6-DMDBT, Fisher, 95%), dimethyldisulfide (DMDS, Aldrich, 99%), and n-octane (Aldrich, 99%).

Results and Discussion

Figure 1 shows the hexagonal structure of Ni_2P. The Ni_2P unit cell has two types of Ni and P sites (denoted as Ni(I), Ni(II) and P(I), P(II)), which form two different trigonal prisms in Ni_2P consisting of various Ni-P and Ni-Ni subshells.

Figure 2 shows the Fourier transforms of the Ni K-edge EXAFS spectra for the freshly prepared samples before reaction and a bulk reference Ni_2P sample. For the bulk Ni_2P the Fourier transform gives two main peaks, a smaller peak at 0.171 nm, and a larger peak at 0.228 nm. For the supported Ni_2P samples there are also two main peaks located at almost the same positions as those of the bulk Ni_2P reference, but with the larger peak weakened and broadened as the surface area of the support increases.

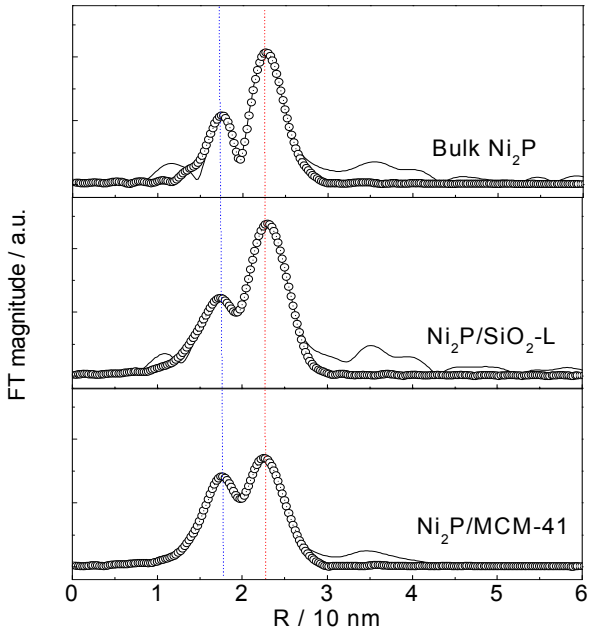

Figure 2. EXAFS analysis results for the fresh samples. The solid lines are the experimental curves and the circles are calculated points.

EXAFS analysis is particularly useful for characterizing the highly dispersed phase on the supports with large surface area. The Feff simulation allowed the assignment of those peaks that appeared in the Fourier transform. The first small peak centered at 0.180 nm was due to P neighbors at 0.2209 and 0. 2266 nm and the second larger peak centered at 0.230 nm was due to a mixed feature of P neighbors at 0.2369 and 0.2457 nm and of Ni neighbors at 0.26783 nm. For the curve fittings the three dominant shells of two Ni-P shells at 0.2266 and 0.2456 nm and one Ni-Ni shell at 0.2678 nm were selected from the simulation results and used as references for phase shift and amplitude calculations. These give reasonable parameters for all samples (Table 1). For example, fitting for the

bulk Ni_2P gives 2 P neighbors at 0.2253 nm and 1.75 P neighbors at 0.2401 nm and 3.99 Ni neighbors at 0.2644 nm. In contrast to bulk Ni_2P, for the supported Ni_2P samples the coordination number of the second shell, Ni-P at 0.2456 nm, increases as dispersion increases, even though the Ni-P bond length decreases. Interestingly, the bond length for the Ni-Ni shell increases with the coordination number as the dispersion increases. It is thus likely that the more dispersed Ni_2P catalyst contains more P atoms, and that the interstitial P atoms lengthen the distance between Ni atoms and weaken the Ni-Ni bond. Ni_2P/MCM-41 containing highly dispersed Ni_2P particles underwent less loss in P, even after the high temperature reduction. This suggests that the smaller particles have a stronger interaction between the Ni and P atoms.

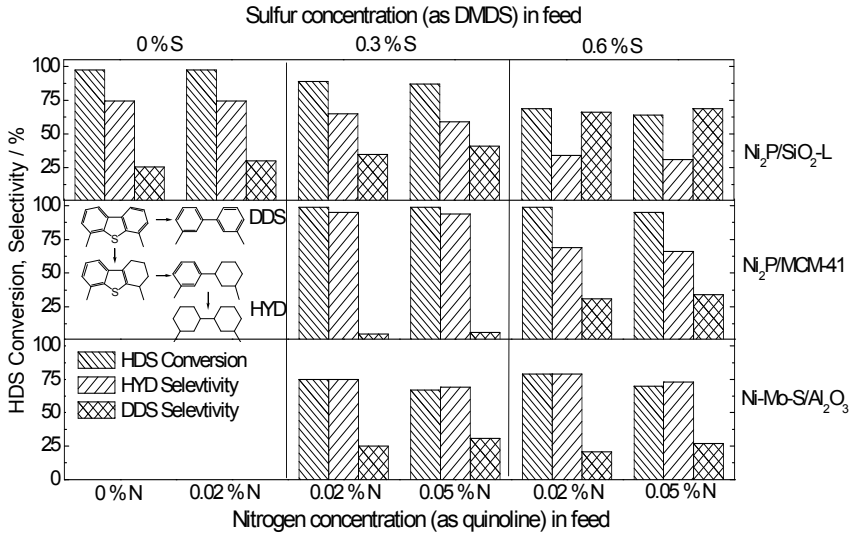

Figure 3. Comparison of hydrogenation/dehydrogenation activity for 4,6-DMDBT over Ni_2P/ SiO_2-L, Ni_2P/ MCM-41 and Ni-MoS/Al_2O_3.

Table 1. Line-Shape Analysis of EXAFS Spectra and Physical Properties of the Supported Ni_2P Catalysts

Samples	Ni-P						Ni-Ni (I, II)			R (%)	CO uptake / mol g^{-1}	BET surface area / m^2 g^{-1}
	Ni-P (I)			Ni-P (II)								
	CN	R	·	CN	R	·	CN	R	·			
Ni_2P Feff reference	2	0.2266		1	0.2369		4	0.2678				
Ni_2P (bulk)	2.0	0.2253	3.00	1.7	0.2401	0.499	3.99	0.2644	6.00	0.48	-	-
Ni_2P / SiO_2-L	1.99	0.2234	4.900	2.6	0.2399	6.352	3.43	0.2612	8.001	0.96	25	88
Ni_2P / MCM-41	1.99	0.2210	2.884	3.5	0.2375	4.361	2.88	0.2631	8.477	1.24	41	487

R filtered = 0.1427 - 0.27598 nm, S_o^2 = 0.9, CN: coordination number, R: bond distance (/nm), : Debye-Waller factor (/ı · nm^2)

Figure 3 compares the conversion and the product selectivities toward direct desulfurization (DDS) and hydrogenation (HYD) of 4,6-DMDBT as a function of nitrogen (as quinoline) and sulfur (as DMDS) content in the feed for the catalysts at 613 K and 3.1 MPa. The catalytic activity for the

catalyst samples in HDS of 4,6-DMDBT followed the order, Ni-MoS/Al_2O_3 < Ni_2P/SiO_2-L < Ni_2P/MCM-41 under 0.35 % S, 0.02 % N, and 1% tetralin. The Ni_2P/MCM-41 showed much better resistance to the inhibition of S and N-compounds with maintenance of higher HDS conversion compared to Ni_2P/SiO_2-L. The EXAFS analysis confirms that the Ni-Ni bond length is widened with dispersion and this feature comes with an increase in Ni-P coordination and a decrease in Ni-P bond length. Thus the higher resistance to the sulfidation can be explained by the stronger interaction between Ni and P species for the highly dispersed Ni_2P catalysts. These results thus suggest that the HDS activity and the resistance to S and N-compound highly depend on the dispersion of the Ni_2P phase.

Conclusions

Nickel phosphide (Ni_2P) catalysts supported on silica and MCM-41 showed high HDS activity for 4,6-DMDBT compared to a commercial Ni-Mo-S/Al_2O_3 catalyst at 573 K (300 ^oC) and 613 K (340 ^oC) and 3.1 MPa based on equal sites (70 μmol) loaded in the reactor. The desulfurization was dominated by the hydrogenation pathway over the Ni_2P catalysts and showed less inhibition by S and N-compounds compared to the sulfide catalysts. Selectivity and performance was higher on the more dispersed catalysts in the order Ni_2P/MCM-41 > Ni_2P/SiO_2-L and this is attributed to the increase in the number of and quality of active sites. Smaller Ni_2P particles have better resistance to S and N compounds due to the stronger interaction between Ni and P in the dispersed Ni_2P phase. EXAFS line shape analysis indicates the formation of a phospho sulfide phase which is favored for the catalysts with shorter Ni-Ni bond length particularly under high S in feed and at relatively high temperature. The phase is responsible for the high activity of the nickel phosphide catalysts.

References

(1) Schlatter, J. C.; Oyama, S. T;. Metcalfe, J. E. ; and Lambert, J. M. *Ind. Eng. Chem. Res*., **1988**, *27*, 1648.
(2) Oyama, S. T. (Ed.), The Chemistry of Transition Metal Carbides and Nitrides; Blackie Academic and Professional: London, 1996.
(3) Robinson, W. R. A. M.; van Gastel, J. N. M.; Korányi, T. I.; Eijsbouts, S. ; van Veen, J. A. R. ; and de Beer, V. H. J., *J. Catal.* **1996**, *161*, 539.
(4) Li, W.; Dhandapani, B.; and Oyama, S. T., *Chem. Lett*. **1998**, 207.
(5) Stinner, C.; Prins, R.; and Weber, Th., *J. Catal.* **2000**, *191*, 438.
(6) Oyama, S. T.; Wang, X.; Lee, Y.-K.; and Requejo, F. G., *J. Catal*. **2002**, *210*, 207.
(7) Oyama, S. T.; Wang, X.; Lee, Y.-K.; and Chun, W.-J., *J. Catal*. **2004**, *221*, 263.
(8) Oyama, S. T., *J. Catal*. **2003**, *216*, 343.
(9) Cheng, C.-F.; Park, D. H.; and Klinowski, J., *J.Chem. Soc., Faraday Trans.*, **1997**, *93(1)*, 193.